

LA-9129-MS

C.3

Los Alamos National Laboratory is operated by the University of California for the United States Department of Energy under contract W-7405-ENG-36.

IS-4 REPORT SECTION

REPRODUCTION
COPY

*...between
...and the
...Cross Section Standard*

LOS ALAMOS NATIONAL LABORATORY



3 9338 00209 7144

Los Alamos Los Alamos National Laboratory
Los Alamos, New Mexico 87545

Photocomposition by Chris West

DISCLAIMER

This report was prepared as an account of work sponsored by an agency of the United States Government. Neither the United States Government nor any agency thereof, nor any of their employees, makes any warranty, express or implied, or assumes any legal liability or responsibility for the accuracy, completeness, or usefulness of any information, apparatus, product, or process disclosed, or represents that its use would not infringe privately owned rights. References herein to any specific commercial product, process, or service by trade name, trademark, manufacturer, or otherwise, does not necessarily constitute or imply its endorsement, recommendation, or favoring by the United States Government or any agency thereof. The views and opinions of authors expressed herein do not necessarily state or reflect those of the United States Government or any agency thereof.

**Differential Cross Sections of the
Reaction ${}^4\text{He}(t,n){}^6\text{Li}$ between
8.5 and 16.5 MeV and the
 $n-{}^6\text{Li}$ Cross-Section Standard**

M. Drosig*
D. M. Drake
R. A. Hardekopf
G. M. Hale

*Visiting Staff Member. Institut Fur Experimental Physik, University of
Vienna, A-1090 Wien, AUSTRIA.



DIFFERENTIAL CROSS SECTIONS OF THE REACTION
 ${}^4\text{He}(t,n){}^6\text{Li}$ BETWEEN 8.5 AND 16.5 MeV AND
THE n - ${}^6\text{Li}$ CROSS-SECTION STANDARD

by

M. Drosig, D. M. Drake, R. A. Hardekopf, and G. M. Hale

ABSTRACT

Differential cross sections of the reaction ${}^4\text{He}(t,n){}^6\text{Li}$, including some data of the first and second excited states of ${}^6\text{Li}$, were measured and compared with an R-matrix analysis of previous data in the ${}^7\text{Li}$ system. Excellent agreement is observed for the angular distribution at the 0.24-MeV resonance of n - ${}^6\text{Li}$, and the shape of the angular distribution for ${}^4\text{He}(t,n){}^6\text{Li}$ at 12.9 MeV is predicted qualitatively by the R-matrix analysis. However, for neutron energies greater than 0.5 MeV for ${}^6\text{Li}(n,t){}^4\text{He}$ the zero-degree excitation function is consistently lower (about 30%) in the R-matrix analysis.

I. INTRODUCTION

Discrepancies in the integrated cross section of the reaction ${}^6\text{Li}(n,t){}^4\text{He}$ have hampered the use of this reaction as a neutron standard for many years.¹ New data around the 0.24-MeV resonance region² using the ${}^3\text{H}(\alpha,{}^6\text{Li})n$ reaction decisively improved the situation in this important energy region. Data of the present work obtained by the ${}^4\text{He}(t,n){}^6\text{Li}$ reaction cover n - ${}^6\text{Li}$ energies between 0.08 and 5.4 MeV. They not only provide new input for further R-matrix analysis of the ${}^7\text{Li}$ system³ but also indicate which of the previous data in this energy range are in error.

II. EXPERIMENT

A. Overview

Differential cross sections of the ${}^6\text{Li}(n,t){}^4\text{He}$ reaction can be obtained not only by detecting the tritons or the α -particles, but also through the inverse reaction

${}^4\text{He}(t,n){}^6\text{Li}$ by detecting the neutrons or the ${}^6\text{Li}$ ions. Therefore, the incoming flux of tritons or alphas can be measured more accurately than can an incoming neutron flux.

Detecting the ${}^6\text{Li}$ ions in the reaction ${}^3\text{H}(\alpha,{}^6\text{Li})n$ gave accurate 0° and 180° cross-section data around the 0.25-MeV resonance.² Because the ${}^6\text{Li}$ ions were produced in the laboratory in a narrow forward cone with a half-angle of only a few degrees, no angular distributions were measured.

Detecting the neutrons in the ${}^4\text{He}(t,n){}^6\text{Li}$ reaction allows a straightforward measurement of the angular distributions. By taking advantage of the quasi-absolute method, accurate absolute differential neutron cross sections can be obtained as was shown for other neutron-producing reactions.⁴ With this method, we use a cross-section standard (preferably of the same reaction) to calibrate the experimental setup. If the experimental conditions are not changed between the calibration and the measurements, the cross-section scale is the same in both cases. Thus most uncertainties cancel, and accuracies greater than 2% can be achieved.⁵

In the present case the accurate 0° data of the reaction ${}^3\text{H}(\alpha, {}^6\text{Li})n^2$ were used as cross-section standards.

Using ${}^4\text{He}(t, n){}^6\text{Li}$ has four advantages.

(1) The projectile has less mass than the target. Therefore neutrons are emitted even at 180° in the laboratory and not only into a forward cone. Only near the threshold, that is, at neutron energies below 0.81 MeV for the $n-{}^6\text{Li}$ interaction, will there be a cone and, consequently, two neutron groups at 0° .

(2) The energy loss of the projectile in the window is less for tritons than for alphas at the same center-of-mass (c.m.) energy. Also, the energy and the angular straggling are less. This fact is important because good energy resolution is needed to measure the sharp resonance (a half-width about 80 keV in the $n-{}^6\text{Li}$ system).

(3) The actual purity of tritium in the target during measurement is very difficult to determine, whereas pure helium is cheap and readily available. This point is important only when additional cross-section standards from other reactions [for example, ${}^2\text{H}(d, n){}^3\text{He}$] are used.

(4) The 0° -reference cross sections have smaller uncertainties than the 180° values.² The latter must be used for the ${}^3\text{H}(\alpha, n){}^6\text{Li}$ reaction.

B. Setup

The triton beam from the tandem Van de Graaff at Los Alamos National Laboratory was bunched to bursts of about a 1-ns time spread with a frequency of 0.625 MHz and a typical average beam current of 10^{-8} A. The helium gas, with an areal density of 0.41 mg/cm², was kept in a 2-cm-long gas cell with an entrance window of 5.4-mg/cm² molybdenum and a gold beam stop. Because of the low beam current, the target was cooled only by an air jet. The pressure in the target and the room temperature were recorded continuously, and the beam current was integrated by a precision digital current integrator.

Neutrons were detected by conventional time-of-flight techniques. See Ref. 6 for information on the detector, its bias setting, and its efficiency.

C. Procedure

A target thickness of 0.41 mg/cm² was chosen so the total energy spread (FWHM) at $E_t = 8.753$ MeV (at the 0.24-MeV resonance for $n-{}^6\text{Li}$) was 92 keV, which is less than the half-width of the resonance (0.12 MeV). At the

highest energy (16.5 MeV), the spread was reduced to 74 keV.

Neutron background from the triton interaction with the entrance foil and the beam stop becomes serious at higher energies. However, this background changes slowly with energy or angle. Therefore, its shape under the neutron line can be determined reliably from neighboring energies and angles, and background can be extracted even for poor signal-to-background ratios caused by the thin target.

The data were taken with two biases simultaneously, namely $1 \times \text{Am}$ (Ref. 6)—about 0.3 MeV of proton energy—and $1 \times \text{Cs}$ (Ref. 6)—about 2 MeV of proton energy. At the higher neutron energies, this method allows a cross-check on the stability of the pulse-height analysis.

Because of the low beam current, beam heating was negligible (less than 0.3%). The deadtime was determined by counting those bursts during which the detector system was busy.

The six data points across the resonance of the 0° excitation function and recent charged-particle data² were used for the absolute calibration of the setup. For this purpose the data were corrected for the energy spread and for effects of the geometrical opening angle on the effective neutron detector efficiency and on the laboratory-to-c.m. conversion.

III. RESULTS AND DISCUSSION

A. Differential Cross Sections for Neutron Production from the Ground State

For comparison with other work and for normalization to the cross-section standard, we have converted our results from laboratory differential cross sections for the reaction ${}^4\text{He}(t, n){}^6\text{Li}$ at $\theta = 0^\circ$ (Table I) to c.m. differential cross sections for the ${}^6\text{Li}(n, t){}^4\text{He}$ reaction at the same angle (Fig. 1). The agreement in shape with the data of Brown *et al.*² across the resonance is excellent. The data of Overlay, Sealock, and Ehlers⁷ were up-scaled by 13%. The data of Rosario-Garcia and Benenson⁸ were down-scaled by 29.5% to agree in scale. Thus the shape of the present excitation function is verified in those two parts. Around 3 MeV the 9.67- and 9.9-MeV levels of ${}^7\text{Li}$ seem to produce some structure in the excitation function, although our data cannot resolve it. Not shown is the prediction of an R-matrix analysis³

TABLE I. ZERO-DEGREE LABORATORY CROSS SECTIONS OF THE REACTION ${}^4\text{He}(t,n){}^6\text{Li}$

E_t (MeV)	${}^4\text{He}(t,n_0){}^6\text{Li}$		${}^4\text{He}(t,n_1){}^6\text{Li}^*$		${}^4\text{He}(t,n_2){}^6\text{Li}^{**}$	
	σ (mb/sr)	Error (%)	σ (mb/sr)	Error (%)	σ (mb/sr)	Error (%)
8.511	31.7	2.5				
8.628	66.9	3.3				
8.708	159	3.1				
8.747	242	2.8				
8.786	193	2.6				
8.979	50.0	2.1				
9.137	38.8	1.9				
9.288	33.3	2.0				
10.488	28.8	1.6				
12.888	21.9	4.7	39.6	1.9		
13.487	24.9	5.8	45.3	4.9		
14.986	27.1	5.7	62.2	3.7	4.0	75
16.457	31.6	8.6	65.2	7.3		

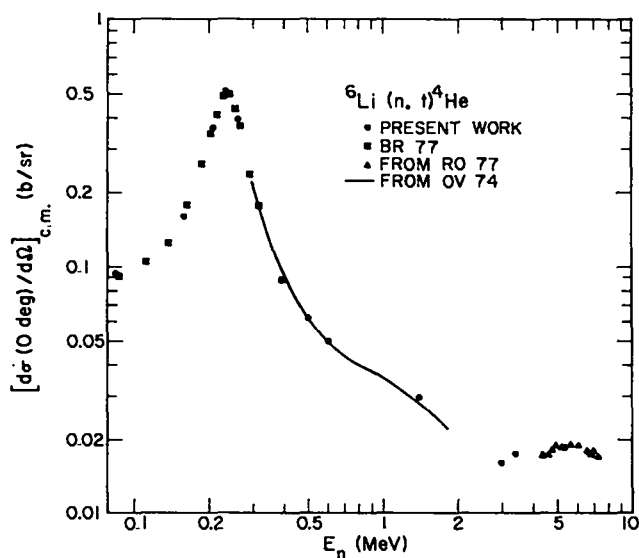


Fig. 1. Zero-degree excitation function for ${}^6\text{Li}(n,t){}^4\text{He}$. The full lines are the scale-adjusted data of Ref. 7; the crosses are those of Ref. 8.

of the ${}^7\text{Li}$ system, which is lower by typically 30% for energies above 0.5 MeV.

Table II summarizes the angular dependence of the differential cross section at 8.747, 12.888, and 16.457

MeV. At 8.747 MeV the neutrons are restricted into a forward cone. The neutron groups from backward c.m. angles are not energetic enough to be recorded in the present experiment. Therefore, only forward-angle data were obtained. The curve in Fig. 2 is an R-matrix prediction that does not include the present data. The agreement is very good, despite a systematic difference in the shape. The ratio of the predicted to the measured cross sections has a tilt of 3% per 40° c.m. The angular distribution at 12.888 MeV (Fig. 3) corresponds to the 2.992-MeV distribution for $n-{}^6\text{Li}$.

Figure 4 gives the angular distributions at 16.457 MeV, which correspond to 5.367 MeV for $n-{}^6\text{Li}$. The R-matrix analysis does not extend to that energy. However, the data of Rosario-Garcia and Benenson⁸ at practically the same energy (5.24 vs 5.37 MeV) agree very well with the present distribution, if their largest angle is excluded and the same scaling factor is applied as for the 0° excitation function.

B. Differential Cross Sections for Neutron Production from Excited States

Table III gives the differential cross sections for the reaction ${}^4\text{He}(t,n_1){}^6\text{Li}^*$ (2.185 MeV) at 12.888 and 16.457 MeV and two data points for ${}^4\text{He}(t,n_2){}^6\text{Li}^{**}$ (3.562 MeV)

TABLE II. ANGULAR DISTRIBUTIONS FOR THE REACTION ${}^4\text{He}(t, n_0){}^6\text{Li}$

$E_t = 8.747 \text{ MeV}$			$E_t = 12.888 \text{ MeV}$			$E_t = 16.457 \text{ MeV}$		
Θ_{Lab} (deg)	σ_{Lab} (mb/sr)	Error (%)	Θ_{Lab} (deg)	σ_{Lab} (mb/sr)	Error (%)	Θ_{Lab} (deg)	σ_{Lab} (mb/sr)	Error (%)
0	242	2.8	0.1	21.9	4.7	0.2	31.5	8.6
3.6	235	3.0	10.0	20.5	5.1	10.0	28.7	10.9
7.3	223	2.9	20.0	21.0	4.4	20.0	22.5	9.3
10.9	199	3.0	30.0	20.1	3.8	30.0	15.5	8.0
14.4	173	2.9	40.0	18.3	5.0	40.0	11.9	6.7
17.8	146	3.0	60.0	10.3	5.1	50.0	8.1	11.3
21.1	123	2.9	80.0	5.2	11.6	60.0	9.2	9.7
24.3	98	3.4	99.2	2.9	11.1	70.0	6.9	7.4
27.2	84	3.7	120.0	2.3	12.2	80.0	4.0	9.7
29.9	85	6.2				90.0	3.2	17.3
						100.0	2.8	20.2
						120.0	2.6	24
						140.0	0.8	78

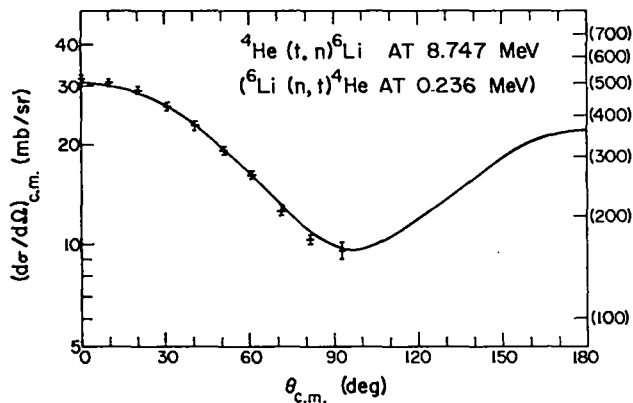


Fig. 2. Angular distribution at 8.747 MeV for ${}^4\text{He}(t, n){}^6\text{Li}$ [at 0.236 MeV for ${}^6\text{Li}(n, t){}^4\text{He}$]. The curve is the R-matrix prediction; the right scale is for $n\text{-}{}^6\text{Li}$.

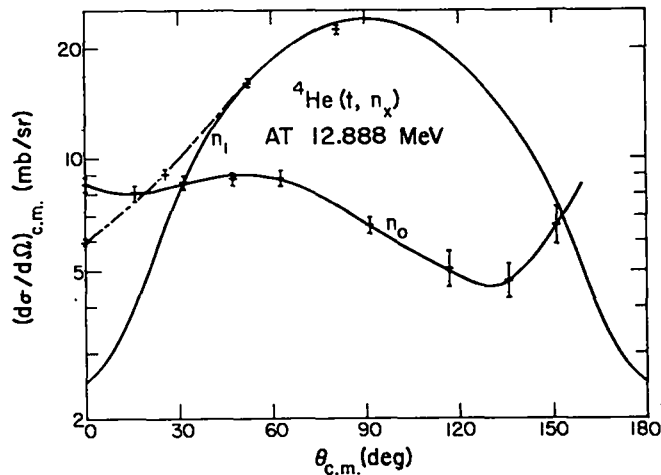


Fig. 3. Angular distributions at 12.888 MeV for ${}^4\text{He}(t, n_x){}^6\text{Li}$ and ${}^4\text{He}(t, n_0){}^6\text{Li}$. * The full curve for n_0 is meant only to guide the eye. The full curve for n_1 is the R-matrix prediction.

at the higher energy. There are no published data for those reactions. The R-matrix analysis³ predicts the salient features at 12.888 MeV: the cross section is peaked at 90° (where even the absolute value is in good agreement). However, the measured 0° value is appreciably higher.

C. Integrated Cross Sections

The discrepancies among the integrated cross sections greater than about 1 MeV (for $n\text{-}{}^6\text{Li}$) are approximately $\pm 25\%$ ¹. Extrapolation of the present data to 180° c.m. does not contribute a large uncertainty to the integrated

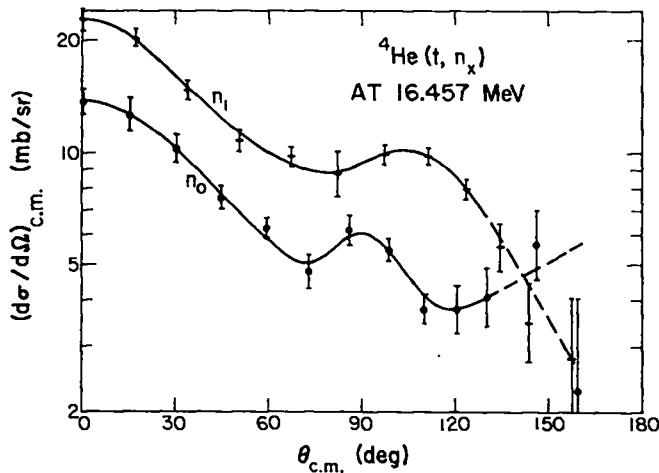


Fig. 4. Angular distributions at 16.457 MeV for ${}^4\text{He}(t, n_1){}^6\text{Li}$ and ${}^4\text{He}(t, n_0){}^6\text{Li}$.* The curves are meant only to guide the eye.

cross sections; at 12.888 MeV we obtain for ${}^4\text{He}(t, n){}^6\text{Li}$ 89 ± 4 mb/sr and for ${}^4\text{He}(t, n){}^6\text{Li}^*$ 217 ± 22 mb/sr. The cross section for the ground state group agrees very well with the recent measurement of Macklin, Ingle, and Harperin⁹ and even with the older data of Murray and Schmitt¹⁰ and Ribe.¹¹ The sum of both cross sections is lower by 19% than that given by Spiger and Tombrello¹² but within their error of 30%.

At 16.457 MeV the integrated cross sections are 74 ± 6 mb/sr for ${}^4\text{He}(t, n){}^6\text{Li}$ and 121 ± 5 mb/sr for ${}^4\text{He}(t, n){}^6\text{Li}^*$. For the ground state reaction Murray and Schmitt¹⁰ obtained 63 ± 6 mb/sr.

D. Energy Uncertainties

From the beginning we intended to use the data of Brown *et al.*,² not only for the cross-section calibration but also for the energy calibration. Therefore, no special calibration of the tandem was needed. Using its nominal energy and the tabulated energy loss¹³ in the entrance window and in half the helium gas, nominal reaction energies were obtained. By matching our 0° excitation function with that of Brown *et al.*,² we found that our nominal energy was high by 12 ± 1.5 keV. Consequently, we reduced our energies by 12 keV. Because the matching could be done with little uncertainty, our energy scale (near the resonance) has the same uncertainty as that of our reference, namely ± 3 keV for $n-{}^6\text{Li}$. For both the energy and the scale adjustment, a knowledge of the energy spread for the energies in the resonance region is important. Whereas the energy straggling in the entrance foil was treated in the Gaussian approximation as in Ref. 2, the target thickness was calculated from the energy loss of the triton beam in the

TABLE III. ANGULAR DISTRIBUTIONS FOR THE REACTIONS ${}^4\text{He}(t, n_1){}^6\text{Li}^*$ and ${}^4\text{He}(t, n_2){}^6\text{Li}^{**}$

$E_t = 12.888$ MeV			$E_t = 16.457$ MeV			n_2	
Θ_{Lab} (deg)	σ_{Lab} (mb/sr)	Error (%)	Θ_{Lab} (deg)	σ_{Lab} (mb/sr)	Error (%)	σ_{Lab} (mb/sr)	Error (%)
0.1	39.6	1.9	0.2	65.6	7.3		
10.0	59.2	3.3	10.0	57.8	5.0	6.3	68
20.0	103	2.8	20.0	40.6	6.1	6.7	36
30.0	142	2.7	30.0	27.6	7.3		
			40.0	22.6	6.4		
			50.0	17.5	15.0		
			60.0	16.3	6.3		
			70.0	12.8	5.9		
			80.0	7.9	6.8		
			90.0	3.9	16.2		
			100.0	1.8	28		
			120.0	0.7	45		

helium gas. Because the resonance is sharp, the correction for finite energy spread is sensitive to the target thickness. We found that the energy-loss tables of Northcliffe and Schilling¹⁴ give energy losses that are too high for tritons in helium. The correctness of the values actually used¹³ was indirectly proved by the fact that all six data points across the resonance are matched simultaneously after correction.

E. Corrections and Errors

The data were corrected for deadtime losses, for the finite energy resolution (around the resonance), and for the effect of the geometrical opening angle on the laboratory-to-c.m. conversion and on the effective energy of the neutrons entering the detector.

The errors shown with the data include statistical errors, background subtraction uncertainties, and uncertainties in the corrections. Also, for neutron energies less than twice the bias energy, a neutron detection efficiency error was included. Above that energy the error in the shape of the (relative) efficiency curve was assumed to be about 2% per 10-MeV energy difference and was not included.

The scale errors are 1.6% at the resonance, 2.3% at 12.9 MeV, and 2.6% at 16.5 MeV. They include the 0.6% error of the reference, an adjustment error of 1.6%, and a contribution from the efficiency curve. In addition, the errors of the integrated cross sections include the uncertainty in the extrapolation to 180°.

F. Comparison with R-Matrix Calculations

The new data provide valuable input for the R-matrix analysis of the ⁷Li system. Several interesting points already are evident when the measurements are compared to existing R-matrix calculations.³

As mentioned previously, the validity of the measurements and the calculations near the $E_n = 0.24$ -MeV resonance is reinforced by their agreement, both in shape and magnitude, at $E_t = 8.747$ (Fig. 2). The normalization of the present measurements corresponds to the higher values seen near the peak of the resonance in recent direct measurements of the ⁶Li(n,t)⁴He integrated cross section.^{9,15} The large disagreements between the calculated and measured 0° ⁶Li(n,t)⁴He cross sections at

energies greater than 0.5 MeV indicate a shape problem, which, considering the accord of the measurements, probably can be attributed to incorrect interference with levels above the resonance in the calculations. Shape problems in the calculated ⁴He(t,n)⁶Li angular distributions may persist to $E_n \sim 3$ MeV ($E_t = 12.888$ MeV), where the experimental indications conflict.

The qualitative agreement between the calculated and measured ⁴He(t,n)⁶Li* cross sections at $E_t = 12.888$ MeV (Fig. 3) confirms the dominance in the $J^\pi = 7/2$ -resonance at $E_x = 9.67$ MeV in ⁷Li of the ²F(t)-⁸P(n₁) transition. This dominance leads to a characteristic $-P_2(\cos \theta)$ dependence on c.m. scattering angle θ that had also been indicated in earlier (³He,P₁) measurements of Spiger and Tombrello.¹² The differences between the calculations and the measurements at small angles indicate that a small admixture of the ⁶P(n₁) state is required in the $J^\pi = 7/2$ -level.

IV. CONCLUSIONS

Measurements of the differential cross sections of the reaction ⁴He(t,n_x) can contribute valuable information about the ⁷Li system and the ⁶Li(n,t)⁴He cross-section standard. Resolution of the structure in the cross section between about $E_t = 2$ MeV and $E_t = 5$ MeV requires smaller steps in energy than those used in this experiment. The target thickness, which limits the energy resolution, should be increased as much as possible to improve the signal-to-background ratio. Then, by using the present technique, data with typically 3% uncertainties should be attainable even at the higher energies.

REFERENCES

1. H. Derrien and L. Edvardson, "Experimental Data Base for the Li-7 System," in *Proc. of the Conf. on Neutron Standards and Applications*, C. D. Bowman et al., Eds., Gaithersburg, Maryland, March 1977 (National Bureau of Standards NBS-Spec. Publ.-493, 1977), p. 14.
2. R. E. Brown, G. G. Ohlsen, R. F. Haglund, Jr., and N. Jarmie, "³H(α ,⁶Li)n Reaction at 0°," *Phys. Rev. C* **16**, 513 (1977).

3. G. M. Hale, "R-Matrix Analysis of the ${}^7\text{Li}$ System," in *Proc. of the Conf. on Neutron Standards and Applications*, C. D. Bowman et al., Eds., Gaithersburg, Maryland, March 1977 (National Bureau of Standards NBS-Spec. Publ.-493, 1977), p. 30.
4. M. Drosig, "Unified Absolute Differential Cross Sections for Neutron Production by the Hydrogen Isotopes for Charged-Particle Energies Between 6 and 17 MeV," *Nucl. Sci. Eng.* 67, 190 (1978).
5. M. Drosig, "Production of Fast Monoenergetic Neutrons by Charged-Particle Reactions Among the Hydrogen Isotopes," in *Proc. IAEA Consultants' Meeting, Neutron Source Properties*, K. Okamoto, Ed., Debrecen, Hungary, March 1980 (International Nuclear Data Committee INDC(NDS)-114/GT, Vienna, 1980), p. 201.
6. M. Drosig, D. M. Drake, and P. Lisowski, "The Contribution of Carbon Interactions to the Neutron Counting Efficiency of Organic Scintillators," *Nucl. Instrum. Methods* 176, 477 (1980).
7. J. C. Overley, R. M. Sealock, and D. H. Ehlers, " ${}^6\text{Li}(n,t){}^4\text{He}$ Differential Cross Sections Between 0.1 and 1.8 MeV," *Nucl. Phys.* A221, 574 (1974).
8. E. Rosario-Garcia and R. E. Benenson, "Neutron-Induced Charged-Particle Reactions in ${}^6\text{Li}$ and ${}^9\text{Be}$," *Nucl. Phys.* A275, 453 (1977).
9. R. L. Macklin, R. W. Ingle, and J. Harperin, " ${}^6\text{Li}(n,\alpha)\text{T}$ Cross Section from 70 to 3000 keV from the ${}^{235}\text{U}(n,f)$ Calibration of a Thin Glass Scintillator," *Nucl. Sci. Eng.* 71, 205 (1979).
10. R. B. Murray and H. W. Schmitt, "Cross Section for the ${}^6\text{Li}(n,\alpha){}^3\text{H}$ Reaction for $1.2 \leq E_n \leq 8.0$ MeV," *Phys. Rev.* 115, 1707 (1959).
11. F. L. Ribe, " ${}^6\text{Li}(n,\alpha){}^3\text{H}$ Cross Section as a Function of Neutron Energy," *Phys. Rev.* 103, 741 (1956).
12. R. J. Spiger and T. A. Tombrello, "Scattering of ${}^3\text{He}$ by ${}^4\text{He}$ and of ${}^4\text{He}$ by Tritium," *Phys. Rev.* 163, 964 (1967).
13. C. F. Williamson, J. P. Boujot, and J. Picard, "Tables of Range and Stopping Power of Chemical Elements for Charged Particles of Energy 0.05 to 500 MeV," Commissariat A L'Energie Atomique report CEA R 3042 (1966).
14. L. C. Northcliffe and R. F. Schilling, "Range and Stopping-Power Tables for Heavy Ions," *Nucl. Data Tables* 7, 233 (1970).
15. C. Renner, J. A. Harvey, N. W. Hill, G. L. Morgan, and K. Rush, "The ${}^6\text{Li}(n,\alpha)$ Cross Section from 80-470 keV," *Bull. Am. Phys. Soc.* 23, 526 (1978).

Printed in the United States of America
 Available from
 National Technical Information Service
 US Department of Commerce
 5285 Port Royal Road
 Springfield, VA 22161
 Microfiche \$3.50 (A01)

Page Range	Domestic Price	NTIS Price Code	Page Range	Domestic Price	NTIS Price Code	Page Range	Domestic Price	NTIS Price Code	Page Range	Domestic Price	NTIS Price Code
001-025	\$ 5.00	A02	151-175	\$11.00	A08	301-325	\$17.00	A14	451-475	\$23.00	A20
026-050	6.00	A03	176-200	12.00	A09	326-350	18.00	A15	476-500	24.00	A21
051-075	7.00	A04	201-225	13.00	A10	351-375	19.00	A16	501-525	25.00	A22
076-100	8.00	A05	226-250	14.00	A11	376-400	20.00	A17	526-550	26.00	A23
101-125	9.00	A06	251-275	15.00	A12	401-425	21.00	A18	551-575	27.00	A24
126-150	10.00	A07	276-300	16.00	A13	426-450	22.00	A19	576-600	28.00	A25
									601-up	†	A99

†Add \$1.00 for each additional 25-page increment or portion thereof from 601 pages up.



Los Alamos